

## Research Article

# Signal Processing for Tracking of Moving Object in Multi-Impulse Radar Network System

**Beom-Hun Kim, Seung-Jo Han, Goo-Rak Kwon, and Jae-Young Pyun**

*Department of Information and Communication Engineering, Chosun University, Gwangju 61452, Republic of Korea*

Correspondence should be addressed to Jae-Young Pyun; [jypyun@chosun.ac.kr](mailto:jypyun@chosun.ac.kr)

Received 2 July 2015; Revised 30 September 2015; Accepted 4 October 2015

Academic Editor: Yuanzhu Chen

Copyright © 2015 Beom-Hun Kim et al. This is an open access article distributed under the Creative Commons Attribution License, which permits unrestricted use, distribution, and reproduction in any medium, provided the original work is properly cited.

Indoor positioning systems (IPs) have been discussed for use in entertainment, home automation, rescue, surveillance, and healthcare applications. In this paper, we present an IPS that uses an impulse radio-ultra-wideband (IR-UWB) radar network. This radar network system requires at least two radar devices to determine the current coordinates of a moving person. However, one can enlarge the monitoring area by adding more radar sensors. To track moving targets in indoor environments, for example, patients in hospitals or intruders in a home, signal processing procedures for tracking should be applied to the raw data measured using IR-UWB radars. This paper presents the signal processing method required for robust target tracking in a radar network, that is, an iterative extended Kalman filter- (IEKF-) based object tracking method, which uses two IR-UWB radars to measure the coordinates of the targets. The proposed IEKF tracking method is compared to the conventional extended Kalman filter (EKF) method. The results verify that the IEKF method improves the performance of 2D target tracking in a real-time system.

## 1. Introduction

Presently, people are familiar with outdoor positioning systems using the global position system (GPS), which does not work indoors. To track moving targets in indoor environments, new tracking systems should be implemented using other sensor/communication methods such as ultrasound, Wi-Fi, infrared, and impulse radio-ultra-wideband (IR-UWB) radar. Indoor positioning systems (IPs) can be used for rescue, surveillance, emergency, and healthcare situations in indoor environments. Generally, object location in indoor environments can be recognized by signals reflected from the target [1]. For high-accuracy target location, we consider an IR-UWB radar-based tracking system in this paper. In addition to its enhanced accuracy, this system possesses several advantages such as high spatial resolution, ultra-low power, and low cost [2, 3]. When these IR-UWB radars are installed on the ceiling of the building, they can monitor the movements of patients in a hospital or intruders in a home. For these surveillance and healthcare applications, the sensor signals observed using IR-UWB radar should be sent to a monitoring server and converted into useful monitoring

signals on the server. That is, radar networks are required for these applications, as shown in Figure 1.

An IR-UWB-based tracking system implemented using a radar network can estimate the distance to the target location by observing the time of arrival (TOA) of the first path, even in the indoor multipath environment. In this paper, we use IR-UWB radar sensor devices for target detection, localization, and tracking of the moving target. The impulse radar consists of two antennas for transmitting and receiving signals. These two antennas exchange an extremely narrow pulse. However, the received target signal is generally perturbed by noise, static clutter, and attenuation. Therefore, we need signal processing procedures for extracting the target signal from the raw delivered radar signals [4]. These procedures consist of (in sequence) clutter reduction, detection, localization, and tracking steps, as shown in Figure 2.

In the clutter reduction step, the primary goal is to remove clutter in the raw data captured by the IR-UWB radar. Because clutter, that is, unwanted signals reflected from static objects in indoor positioning applications, is present, the received signal (which includes clutter) should be carefully handled [5]. We applied the conventional Kalman filter- (KF-)

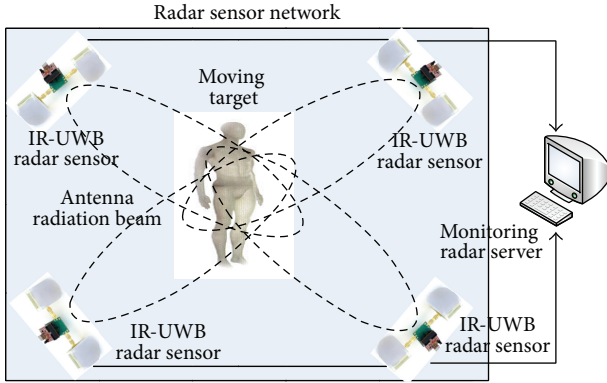


FIGURE 1: Radar sensor network for surveillance and healthcare applications.

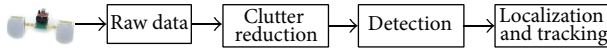


FIGURE 2: Signal processing procedures in IR-UWB application.

based clutter reduction method, which is known to be the best among the conventional methods such as exponential average (EA), singular value decomposition (SVD), and Kalman filter (KF) [6].

In the detection step, the location of the target is determined. First, the strength of the clutter-eliminated signal is compared to a threshold. If the signal strength is greater than the threshold, a target is considered to be present. There are detection techniques such as CLEAN, modified CLEAN, matched filter, and constant false alarm rate (CFAR) [7, 8]. In this paper, we use a modified CLEAN method for the detection step introduced in the previous work [8]. The modified CLEAN method searches all pulse presences by the cross-correlation between the received signal and the template signal and then compares them to a threshold. However, the received signal strength will be weaker when the target distance is greater. Therefore, the modified CLEAN compensates the weak signal transferred from the faraway target and detects the target presence based on 1D/2D based window method. That is, the filtering method is applied in this detection stage.

In the localization and tracking step, the distance to the target is determined using the TOA of the detected target signal. Indeed, the distance to the target is obtained by multiplying the target sample index with the sample resolution of IR-UWB radar. However, there are still estimation errors in the target location. To localize and track the moving target, several methods such as trilateration, Kalman filtering (KF), and extended KF (EKF) have been proposed [9, 10].

The KF-based tracking used in this method has good performance for linear systems. However, this technique has high estimation errors because of the nonlinear relationship between measurements and system states. On the other hand, EKF has better performance than the conventional KF-based tracking method in the nonlinear estimation system. However, the conventional method still has low estimation

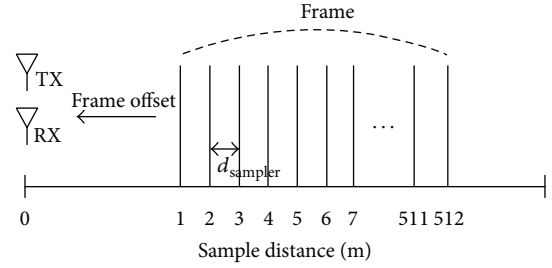


FIGURE 3: The frame construction of IR-UWB radar.

features for tracking because the measurement noise and error covariance matrix in EKF are affected by underestimating the (substantial) covariance matrices. Additionally, if the initial state estimation is wrong, this filter could diverge rapidly because of its linearization. As a result, the accuracy of tracking performance in EKF can be reduced when the target drastically changes its direction.

In this paper, we present a performance evaluation of the proposed iterative EKF- (IEKF-) based target tracking method. IEKF has been introduced in our previous work; however, in this paper, it is extensively illustrated and analyzed in a radar network at its suggested radar positions; we provide various experimental results [11]. IEKF uses a recursive estimation procedure to determine an object's motion parameters based on a series of signals. Thus, this method can estimate the target position for drastic direction changes of moving targets better than EKF can. Using IEKF, we estimate the target trajectories in both natural and drastic movements of a target.

The remainder of this paper is organized as follows: Section 2 presents the conventional location estimation methods that can be useful in 2D radar monitoring system. Then, Section 3 describes the conventional EKF- and proposed IEKF-based location estimation method. The proposed and conventional target tracking radar methods are compared in Section 4 based on experimental results. Finally, the conclusions of this work follow, in Section 5.

## 2. Location Estimation Methods

To track the moving object using the IR-UWB radar system, we perform the steps of clutter reduction and detection. Then, the location of the target should be determined from the target-detected signal samples.

This paper uses IR-UWB radar with NVA6100 chipset developed by Novelda [12]. Figure 3 shows a frame structure consisting of samples captured at IR-UWB radar receiver. The one frame consists of the 512 samples in this paper work. Thus, sample can be interpreted to signal propagation time and target distance. In the condition of 512 samples per frame, the time interval of each sample is set up to 27 ps. The distance from radar to the target,  $d_{\text{sampl er}}$ , could be expressed with the interval,  $\text{sample\_interval}$  time, shown in (1).  $C$  is the radio wave speed in air. Consider

$$d_{\text{sampl er}} = \frac{C \times \text{sample\_interval time}}{2}. \quad (1)$$

By using (1), the resolution of the observed distance could be about 4 millimeters. That is, the 512 samples can measure about 2 meters. To measure a distance over the 2 meters, the UWB radar system delays sampling times as long as the target locates.

Therefore, the target signal samples indicating the target location can be converted into the distance to the target. To obtain the target distance, we use

$$D = N \times R, \quad (2)$$

where  $N$  is the target signal sample index of a frame stored after applying the detection technique and  $R$  is the sample resolution, 4 mm in our work. For example, if  $N$  is 500, then  $D$  is 2m.

For the radar monitoring network, we use two impulse radars, which determine the target location in 2D coordinates. Therefore, the distance determination can be expressed by a two-circle intersection as follows:

$$(dx - X_i)^2 + (dy - Y_i)^2 = r_i^2 \quad (i = 1, 2). \quad (3)$$

$X_i$  and  $Y_i$  are the  $x$  and  $y$  coordinates of the radar positions, respectively, where  $i$  is the number of the radar.  $dx$  and  $dy$  are the  $x$  and  $y$  coordinates of the target locations from each radar.  $r_i$  is a radius to target from the radar. Each target distance makes a circle with a radius measured from the radar position to the target locations as shown in Figure 4. Here, we can find the target location which is the coordinate of intersection that these circles make. But the number of intersections is at least two. In Figure 5, we could know that the intersection occurring on the first quadrant is only valid for a target location, when the radiation angle is shown depicted with the blue arrows in the figure. That is, one intersection of circles existing on the first quadrant and residing in the area overlapped by two radar RF signals is selected from two intersections. If two intersections are still available in the intersection selection, the intersection close to the previous observed location is preferred. However, the observed target distance information still contains noise: therefore, an additional filtering method is needed for location estimation. For high-performance location estimation, linear and nonlinear approaches can be used. Linear systems are used for predictable cases in location estimation. When using a linear system, the current distance of the target is estimated from the previous location in a linear manner, whereas nonlinear systems use nonlinear formulas to estimate the current target location.

In our experiments, we carried out location estimation using EKF and IEKF to track a moving target, where the EKF and IEKF estimation methods are governed by nonlinear systems [13]. These two estimation methods provide the current target location in 2D coordinates using nonlinear estimation approaches. The system model  $x$  and measurement model  $z$  are described as follows:

$$x_k = f(x_{k-1}, u_{k-1}) + w_{k-1}, \quad (4)$$

$$z_k = h(x_k) + v_k, \quad (5)$$

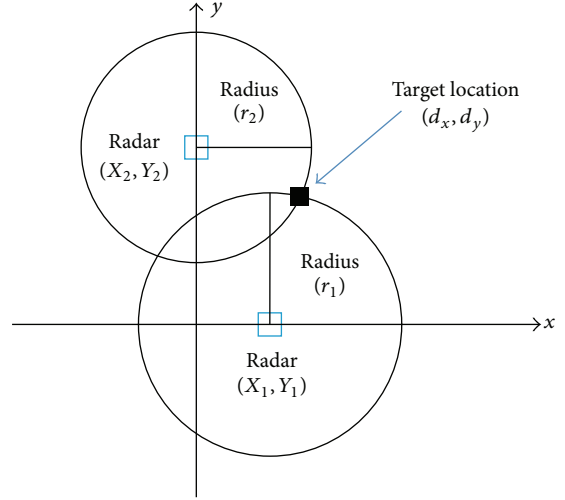


FIGURE 4: Intersection of two circles.

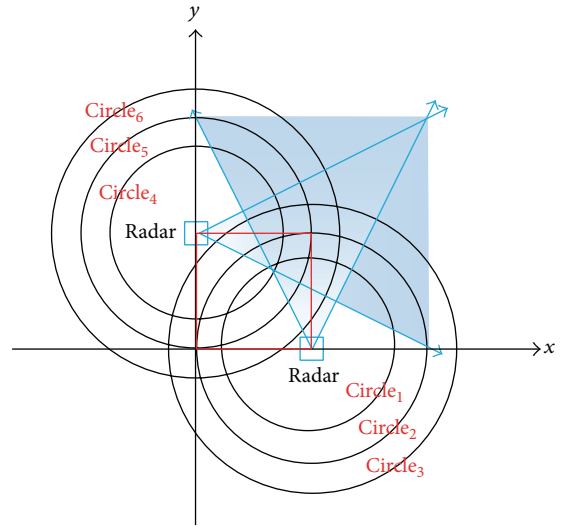


FIGURE 5: Target estimation based on intersection position and radar radiation angle.

where  $k$  is a time index,  $u$  is the control input such as an acceleration,  $w$  is the process noise, and  $v$  is the measurement noise. When applying the estimation methods, we must define the appropriate target state vector in these methods as follows:

$$x_k = [dx, vx, dy, vy]^T, \quad (6)$$

where  $dx$  is the  $x$ -coordinate location,  $dy$  is the  $y$ -coordinate location, and  $v$  is the velocity of the target.

**2.1. EKF Estimation for 2D Target Tracking.** The EKF state model is the same as the KF state model because EKF is a nonlinear version of KF. The EKF state model is made of the motion estimation for the target, which is needed by the tracking system. Consider

$$x_k = f(x_{k-1}, u_{k-1}) + w_{k-1} = Ax_{k-1} + Bu_{k-1} + w_{k-1}. \quad (7)$$

First, we derive the state and measurement model. Equation (7) is the state model in KF, EKF, and IEKF. This state model can be changed by the target state vector for estimation as follows:

$$x_k = \begin{bmatrix} dx_k \\ vx_k \\ dy_k \\ vy_k \end{bmatrix} = \begin{bmatrix} dx_{k-1} + vx_{k-1}t + a_x \frac{t^2}{2} \\ vx_{k-1} + a_x t \\ dy_{k-1} + vy_{k-1}t + a_y \frac{t^2}{2} \\ vy_{k-1} + a_y t \end{bmatrix} + w_{k-1}, \quad (8)$$

where  $w_k = \mathcal{N}(0, Q)$  is the additive process noise with covariance matrix  $Q$ . The transition matrix  $A$  is given by

$$A = \begin{bmatrix} 1 & t & 0 & 0 \\ 0 & 1 & 0 & 0 \\ 0 & 0 & 1 & t \\ 0 & 0 & 0 & 1 \end{bmatrix}, \quad (9)$$

where  $t$  is 1. The control input matrix  $B$  is given by

$$B = \begin{bmatrix} \frac{t^2}{2} & 0 & 0 & 0 \\ 0 & t & 0 & 0 \\ 0 & 0 & \frac{t^2}{2} & 0 \\ 0 & 0 & 0 & t \end{bmatrix}. \quad (10)$$

The input vector  $u$  is given by

$$u_k = \begin{bmatrix} a_x \\ a_x \\ a_y \\ a_y \end{bmatrix}, \quad (11)$$

where  $a_x$  and  $a_y$  are the acceleration components of the target. Additionally, we derived the EKF measurement model as follows:

$$z_k = \begin{bmatrix} r_1 \\ r_2 \end{bmatrix} = \begin{bmatrix} \sqrt{(dx - X_1)^2 + (dy - Y_1)^2} \\ \sqrt{(dx - X_2)^2 + (dy - Y_2)^2} \end{bmatrix} + v_k, \quad (12)$$

where  $X_1, X_2, Y_1,$  and  $Y_2$  are the locations of each radar in the  $x$  and  $y$  coordinates, as shown in Figure 4.

Second, we present the estimation process, which consists of prediction and correction steps. The previously mentioned problem is how to transform the nonlinear target state vector into the linear target state vector. In EKF, this problem has been resolved using a Jacobian matrix [13]. The EKF algorithm recursively carries out prediction and correction steps in the following order:

$$\text{initialize: } \hat{x}_{k-1}^-, P_k^- \quad (13)$$

$$\hat{x}_k^- = Ax_{k-1} + Bu_{k-1}, \quad (14)$$

$$P_k^- = AP_{k-1}A^T + Q, \quad (15)$$

$$K_k = P_k^- H_k^T (H_k P_k^- + R)^{-1}, \quad (16)$$

$$\hat{x}_k = \hat{x}_k^- + K_k (z_k - h(\hat{x}_k^-)), \quad (17)$$

$$P_k = (I - K_k H_k) P_k^-. \quad (18)$$

The prediction step operates as shown in (13), (14), and (15).  $\hat{x}_{k-1}^-$  is the state vector and  $P_k^-$  is the error covariance diagonal matrix, which is the same size as the number of state vectors. In (14), the current location is predicted using  $x_{k-1}$ . Also,  $P_k^-$  is updated by  $P_{k-1}$  and  $Q$  to obtain the next estimated location.  $Q$  is the process noise covariance diagonal matrix, which is the same size as the number of state vectors:

$$Q = \begin{bmatrix} q_k & 0 & 0 & 0 \\ 0 & q_k & 0 & 0 \\ 0 & 0 & q_k & 0 \\ 0 & 0 & 0 & q_k \end{bmatrix}, \quad (19)$$

where  $q$  is the variance of each process noise, as defined by the user. The correction method is shown in (16), (17), and (18); it is used for computing the Kalman gain, updating the estimation state, updating the error covariance, and computing the Jacobian matrix. The Jacobian matrix is as follows:

$$H_k = \begin{bmatrix} \frac{\partial h_1}{\partial x_k} \\ \frac{\partial h_2}{\partial x_k} \end{bmatrix} = \begin{bmatrix} \frac{dx_k - X_1}{\sqrt{(dx_k - X_1)^2 + (dy_k - Y_1)^2}}, 0, \frac{dy_k - Y_1}{\sqrt{(dx_k - X_1)^2 + (dy_k - Y_1)^2}}, 0 \\ \frac{dx_k - X_2}{\sqrt{(dx_k - X_2)^2 + (dy_k - Y_2)^2}}, 0, \frac{dy_k - Y_2}{\sqrt{(dx_k - X_2)^2 + (dy_k - Y_2)^2}}, 0 \end{bmatrix}. \quad (20)$$

In (16),  $R$  is the measurement noise covariance matrix, which has the same size as the number of radars, as follows:

$$R = \begin{bmatrix} c_k & 0 \\ 0 & c_k \end{bmatrix}, \quad (21)$$

where  $c$  is the variance value of each measurement noise, as defined by the user. In (18),  $I$  is the identity matrix [13].

**2.2. IEKF Estimation for 2D Target Tracking.** Generally, EKF is used to localize and track a moving target. Sometimes EKF has low tracking performance, such as when the trajectory of the target drastically changes. This happens because EKF uses fixed initial filter parameters. To improve this weakness of EKF, IEKF includes a recursive strategy that iteratively calculates certain filter parameters; in this strategy, IEKF defines an iteration triggering threshold based on the difference between the current estimated location and the previous estimated location. This triggering threshold is defined as 0.01 by experimental experience. If the difference value is larger than the predefined threshold, the added iterative function restarts to obtain the current location using a randomly chosen measurement noise covariance  $R$  [14, 15]. This added strategy allows the target tracking system to operate in a wide variety of target movement situations.

IEKF uses the same state model and measurement model as EKF; it also uses the same prediction and correction steps as EKF. The prediction step of IEKF is the same as that of EKF. However, the correction step of IEKF adds an iterative process to that of EKF. The correction step of IEKF uses the following four processes. First, Jacobian matrix  $H_k$  is computed to update the Kalman gain. Second, the Kalman gain  $K_k$  is computed using the Jacobian matrix  $H_k$  and measurement noise covariance  $R$ . The value of  $R$  is randomly chosen whenever repeated before updating the Kalman gain in this improved strategy. Third, the method estimates the next location as follows:

$$\hat{x}_n = \hat{x}_k^- + K_n(z_n - h(\hat{x}_n^-) - H(\hat{x}_k^- - \hat{x}_n)), \quad (22)$$

where  $n$  is the iteration count in the added function; it increases by one, from zero. If the difference between the estimated next location  $\hat{x}_n$  and current location  $\hat{x}_k^-$  is bigger than the predefined threshold,  $n$  increases one and (22) is refreshed. These three processes are the added iterative strategy. Last, error covariance  $P_k$  is updated like (18). The measurement noise covariance  $R$  has an effect on the estimation results because of the change of  $R$  [11].

When we compare EKF and IEKF, the difference is whether the measurement noise covariance  $R$  is continuously changed or not. This difference indicates that IEKF can be useful in a variety of tracking conditions. That is,  $R$  of IEKF is adaptively changed to obtain results with higher accuracy.

### 3. Experimental Scenario

To perform experiments for moving target tracking over a multi-impulse radar network, we use one monitoring server, two IR-UWB radar sensor devices with the NVA6100 chipset

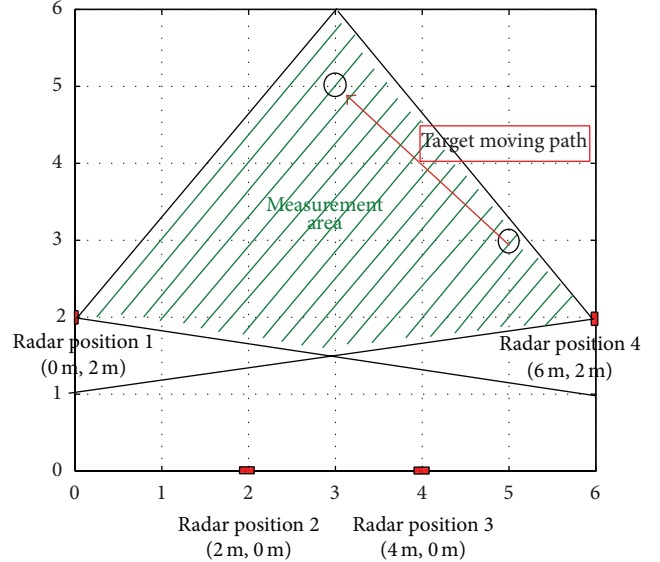


FIGURE 6: The measurement area generated by the antenna angles of the selected radars. In this example, positions 1 and 4 are chosen (first experiment).

TABLE 1: The average distance to the starting and ending positions of target movement from radars.

Radar position	Start position	End position
Case 1	4.67 m	4.67 m
Case 2	4.13 m	4.67 m
Case 3	3.26 m	4.24 m

developed by Novelda, and sinusoidal directional (TX and RX) antennas with an opening angle of 42 degrees [16]. The radars are set up to work pulse repetition frequency at 48 MHz and radar-scan rate of approximately 24 radar-scans per second. The transmitted pulse width is 0.7 ns and the frequency range is from 3.1 GHz to 5.6 GHz. Also, its power spectral density limit is  $-41.3$  dBm/MHz indoors and outdoors. Two IR-UWB radar devices are connected to the monitoring server, which performs signal processing for target localization and tracking. The radars observe a target located 8 m away in our experimental condition. Also, the target moves with a speed of 0.3 meters per second in our experiments. EKF- and IEKF-based localization and tracking methods were used for experiments in an indoor environment of  $6\text{ m} \times 6\text{ m}$  in area. To obtain the coordinates of the target, the constant target and moving target were designed to move or hold within the observation area, which is covered by two IR-UWB radars, as shown in Figure 6.

First, we carried out tests by changing the position of the radar to obtain the best placement of radars. In the first test (case 1, shown in Table 1), the two radars are located at (2 m, 0 m) and (0 m, 2 m), where  $(x, y)$  indicates the  $x$  and  $y$  positions on a coordinate plane. In the second test (case 2), the two radars are located at (4 m, 0 m) and (0 m, 2 m). In the last test (case 3), the two radars are relocated at (6 m,



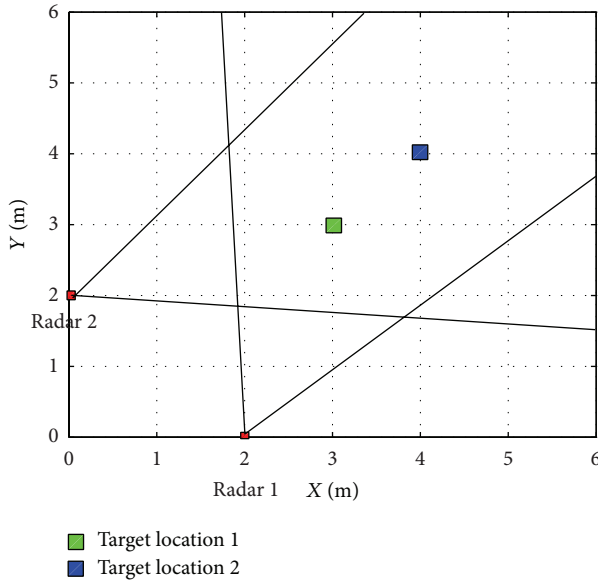


FIGURE 7: The locations of the fixed targets for the second experiment when the two radars are located at (0 m, 2 m) and (2 m, 0 m).

2 m) and (0 m, 2 m). Under these conditions, the target moves from (5 m, 3 m) to (3 m, 5 m), as shown in Figure 6.

Second, we carried out filtering performance experiment at the two different locations such as (3 m, 3 m) and (4 m, 4 m) localization shown in Figure 7. In this experiment, the two radars are positioned in the selected locations such as (2 m, 0 m) and (0 m, 2 m) and evaluated with the proposed IEKF-based target localization method.

Third, we carried out the last experiment with the two trajectories shown in Figure 8. In this experiment, the two radars are positioned in the same locations as the second experiment and evaluated with the proposed IEKF-based target tracking method.

## 4. Experimental Results

*4.1. Selection of Radar Location.* In these experiments, the observed raw signals are conveyed to the server and reinterpreted by the KF clutter reduction and modified CLEAN detection steps.

In the first experiment, we tested the three cases of different radar locations, as shown in Figures 9, 10, and 11. These figures show the orthogonal setup for the position of two radars to monitor a confined area [17]. In Figure 9, the two radars are located at (2 m, 0 m) and (0 m, 2 m), and a target moves from (5 m, 3 m) to (3 m, 5 m). The test of case 1 shows the worst tracking result among the three cases, because the distances from the radar antennas to the target are the longest among the cases. Table 1 gives the average distance to the starting and ending positions of the target movement. As we expected, the distance to the target determines the accuracy of tracking, even when the tracking filters are applied. The tests of cases 2 and 3 show better location estimation with this target tracking method, because the distances from the radars to the target

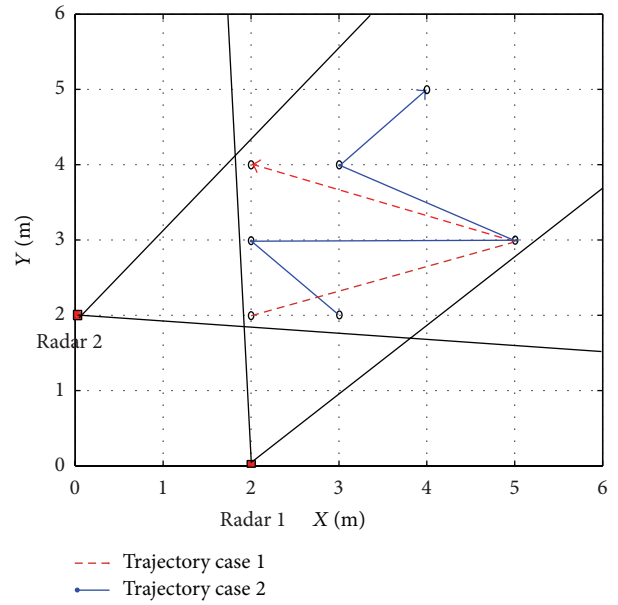


FIGURE 8: The trajectories of the moving target when the two radars are located at (0 m, 2 m) and (2 m, 0 m).

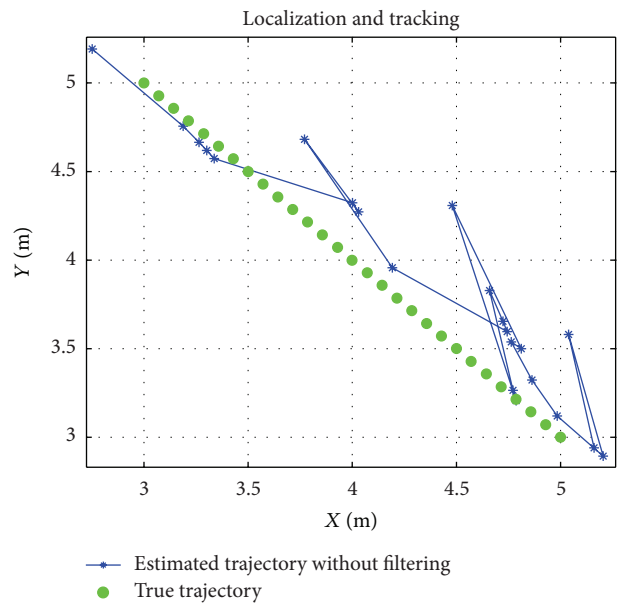


FIGURE 9: Estimated tracking results of the moving target in 2D coordinates when the radars are located at (2 m, 0 m) and (0 m, 2 m).

are shorter than that of case 1. Therefore, we can conclude that the location closer to the target is preferred for the impulse radar position. However, if targets move randomly in the experiment area, any selection of radar positions is acceptable. In this work, we chose case 1 to provide good and bad signal detection conditions for our radar position. Our developed radar system is to be evaluated and compared to conventional systems in various experimental environments. Figure 12 demonstrates how the tracking system determines

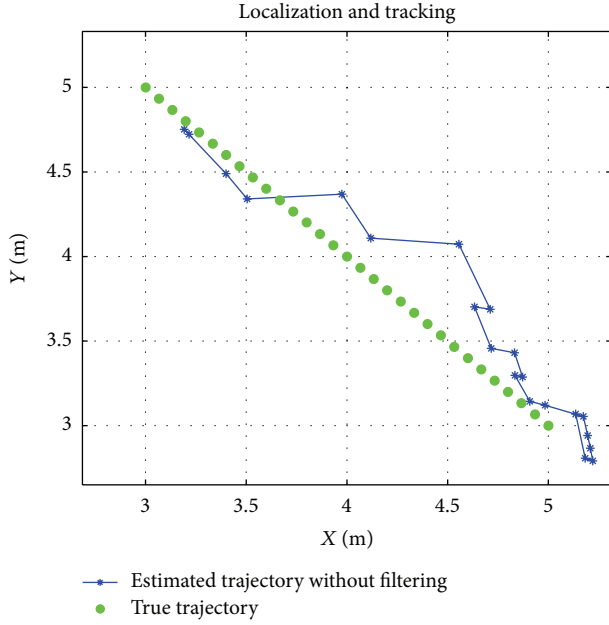


FIGURE 10: Estimated tracking results of the moving target in 2D coordinates when the radars are located at (4 m, 0 m) and (0 m, 2 m).

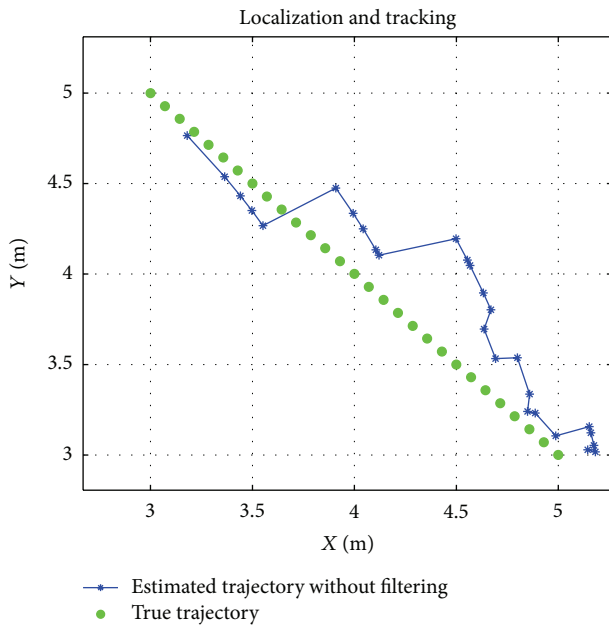


FIGURE 11: Estimated tracking results of the moving target in 2D coordinates when the radars are at (6 m, 2 m) and (0 m, 2 m).

the route of a moving target when the radars are positioned as they are in case 1.

**4.2. The Performance Evaluation of IEKF and EKF Filtering Methods.** In the second and third experiments, IEKF and EKF filtering methods are used for the localization and tracking estimation of a fixed and moving target. We tested two localization cases and two trajectories, as shown in Figures 7 and 8. In these experiments, we fixed the radar locations at

TABLE 2: Performance comparison of filtering methods for fixed target located on (3 m, 3 m).

Method	RMSE	Covariance $R$
Without filtering	0.1368	None
EKF	0.1312	$c = 0.01$
EKF	0.1232	$c = 0.05$
EKF	0.1184	$c = 0.1$
EKF	0.1068	$c = 0.5$
IEKF	0.0938	$c$ is randomly chosen

TABLE 3: Performance comparison of filtering methods for fixed target located on (4 m, 4 m).

Method	RMSE	Covariance $R$
Without filtering	0.3311	None
EKF	0.2983	$c = 0.01$
EKF	0.2561	$c = 0.05$
EKF	0.2319	$c = 0.1$
EKF	0.1771	$c = 0.5$
IEKF	0.1356	$c$ is randomly chosen

TABLE 4: Performance comparison of different localization and tracking methods for trajectory case 1.

Method	RMSE	Covariance $R$
Without filtering	0.2478	None
EKF (1)	0.2373	$c = 0.01$
EKF (2)	0.2321	$c = 0.05$
EKF (3)	0.2373	$c = 0.1$
EKF (4)	0.3373	$c = 0.5$
IEKF (1)	0.2270	$c$ is randomly chosen
IEKF (2)	0.2285	$c$ is randomly chosen
IEKF (3)	0.2289	$c$ is randomly chosen
IEKF (4)	0.2289	$c$ is randomly chosen

(2 m, 0 m) and (0 m, 2 m). To localize the constant target and to track the moving target, we used KF clutter reduction and modified CLEAN detection techniques on the raw data before starting the localization and tracking signaling process. Then, we adopted IEKF and EKF filtering methods for the fixed and moving object. In these experiments, when the variance of measurement noise  $c$  in the EKF filtering method is changed from 0.01 to 0.5, the root mean square error (RMSE) between the estimated position and trajectory is seen to be different each time. However, in the case of the IEKF filtering method, the coefficient  $c$  is randomly chosen and updated at each iteration. The estimated localization and tracking results are depicted in Figures 13, 14, 15, 16, 17, and 18.

The results of the second experiment are shown in Tables 2 and 3 with the RMSE between the estimated localization and true position. As can be seen in the results, the IEKF filtering method has the better RMSE values of 0.0938 and 0.1356, whereas the EKF has RMSE values of 0.1068 and 0.1771 for the two localization experiments, respectively. In the third experiment result, Tables 4 and 5 show RMSE between the

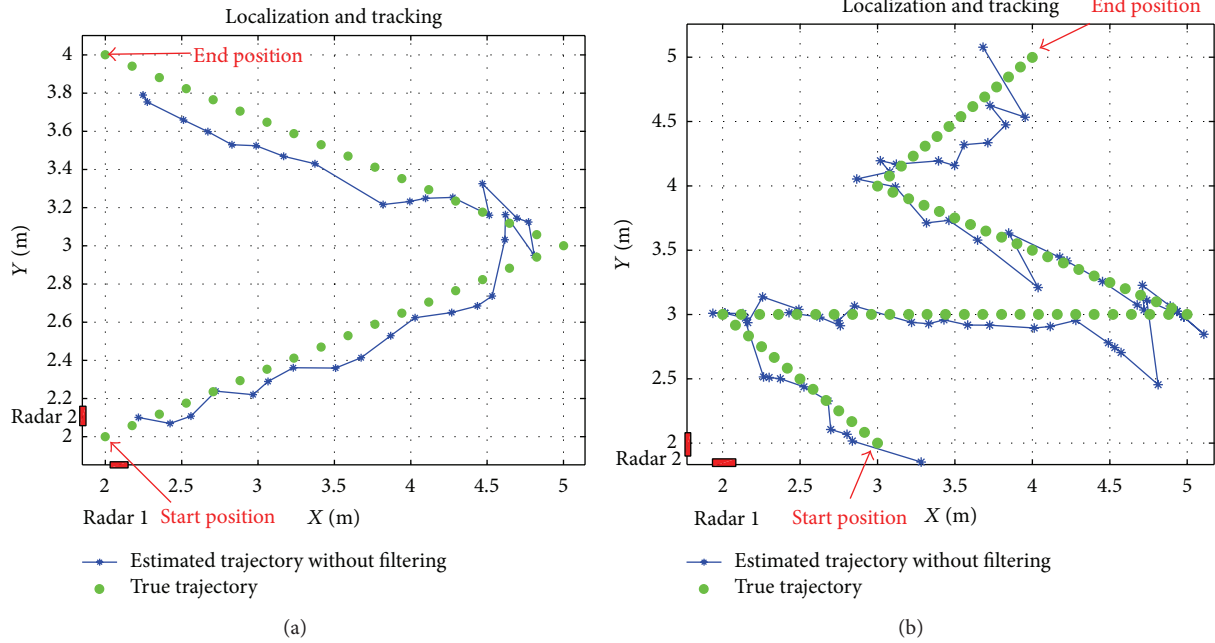


FIGURE 12: Estimated tracking results of the moving target in 2D coordinates in the case of no filtering, (a) first trajectory, (b) second trajectory.

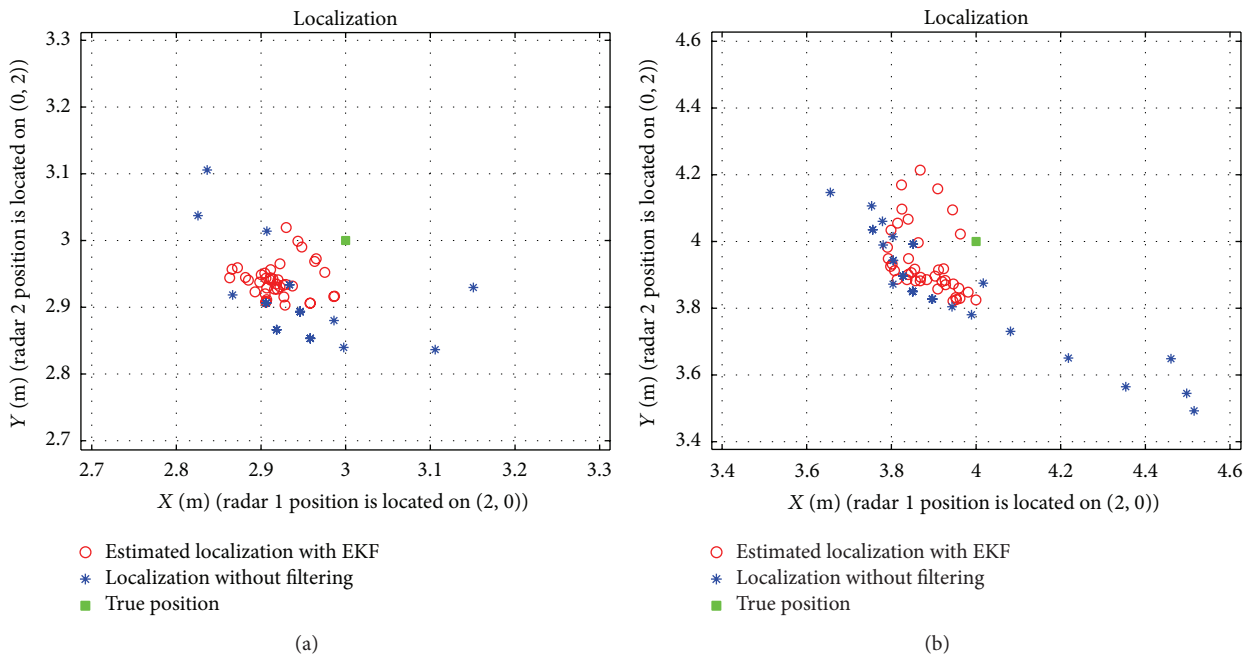


FIGURE 13: Estimated localization result of fixed target using EKF filtering with  $c$  of 0.5, (a) target location of (3 m, 3 m) and (b) target location of (4 m, 4 m).

estimated trajectories and true trajectories using two filtering methods. As a result, the IEKF filtering method has better RMSE values of 0.2270 and 0.2145, whereas the EKF has RMSE values of 0.2321 and 0.2378 for the two trajectory experiments, respectively.

As our results show, the proposed IEKF filtering method tracks closer to the real target position than the EKF filtering method does under the different covariance condition.

Therefore, the value of the covariance  $R$  is shown affecting the tracking result. A large covariance  $R$  generally increases the range of estimation error, whereas a small covariance  $R$  decreases the range of estimation error. However, the smallest covariance  $R$  does not always decrease the range of the estimation error, as shown in Tables 2, 3, 4, and 5. We can conclude that the EKF filtering method using a constant covariance  $R$  is not adaptive in a variety of indoor



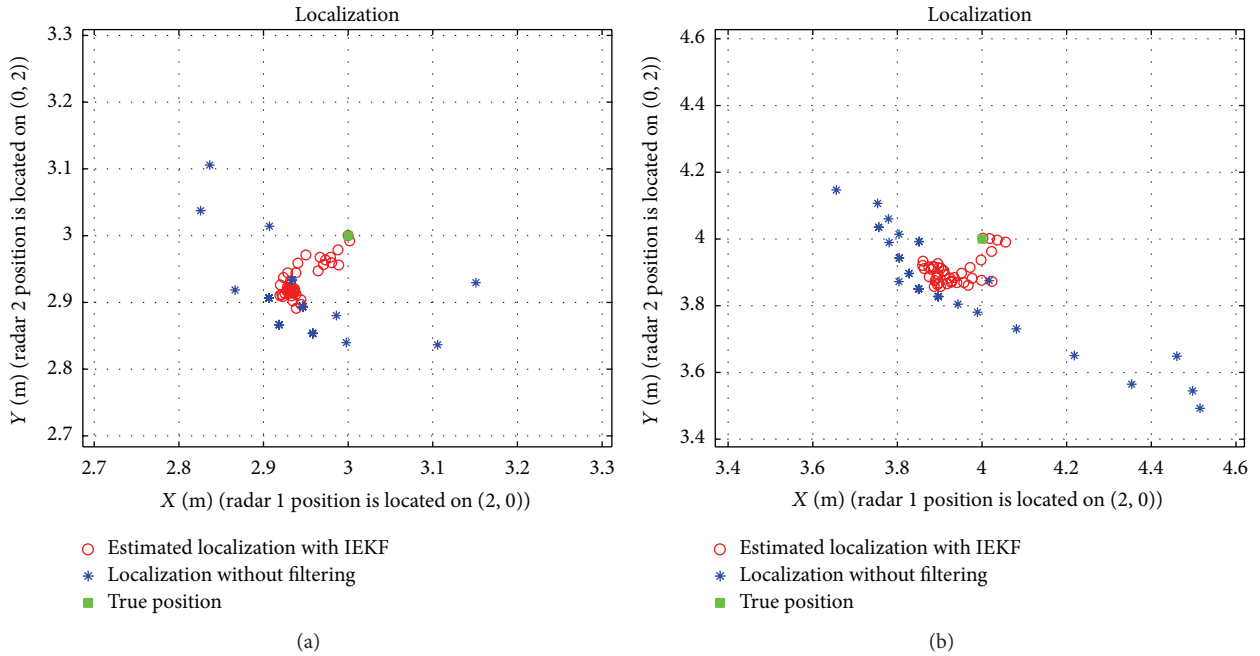


FIGURE 14: Estimated localization result of fixed target using IEKF filtering, (a) case 1 and (b) case 2.

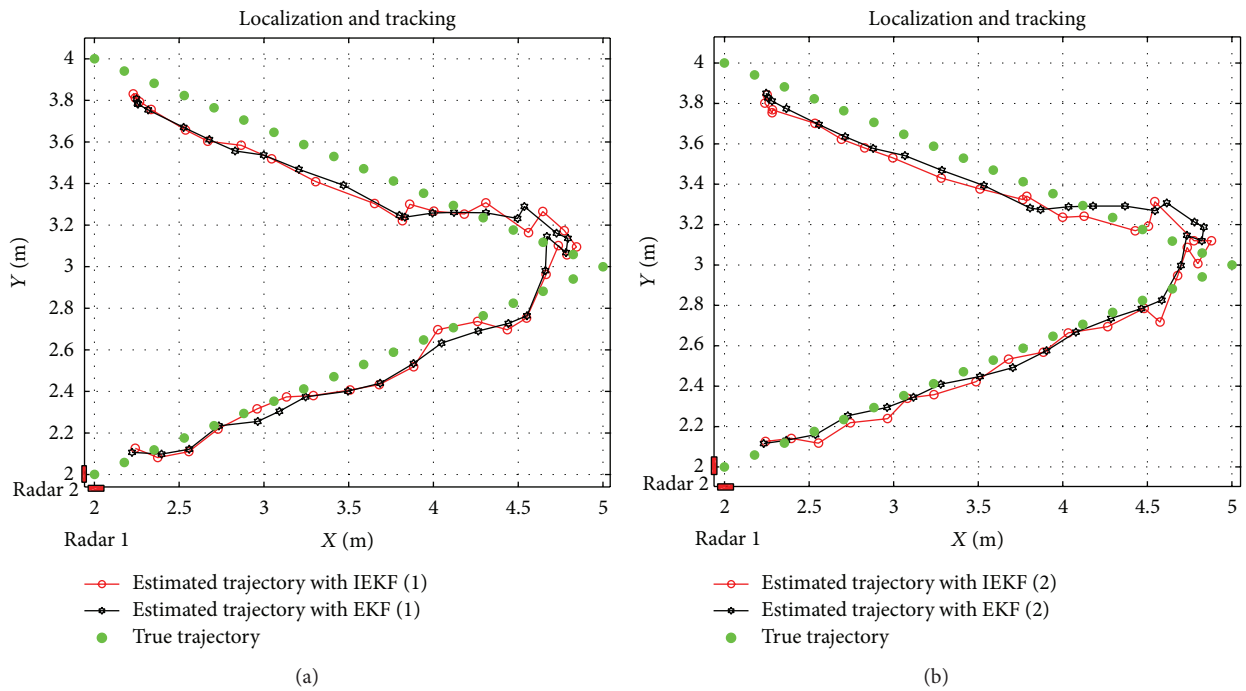


FIGURE 15: Estimated tracking result of moving target in 2D coordinates in the case of EKF and IEKF filtering methods, (a) EKF using  $c = 0.01$  and (b) EKF using  $c = 0.05$ .

environments [8]. However, the IEKF filtering method can be used in a robust target tracking system because the covariance  $R$  is changeable. When the various trajectories of the target are tracked, the IEKF filtering method can find the appropriate covariance  $R$ .

## 5. Conclusion

In this paper, we discussed the signal processing technologies required for a target localization and tracking system using an IR-UWB radar network. Tracking of a moving target is the

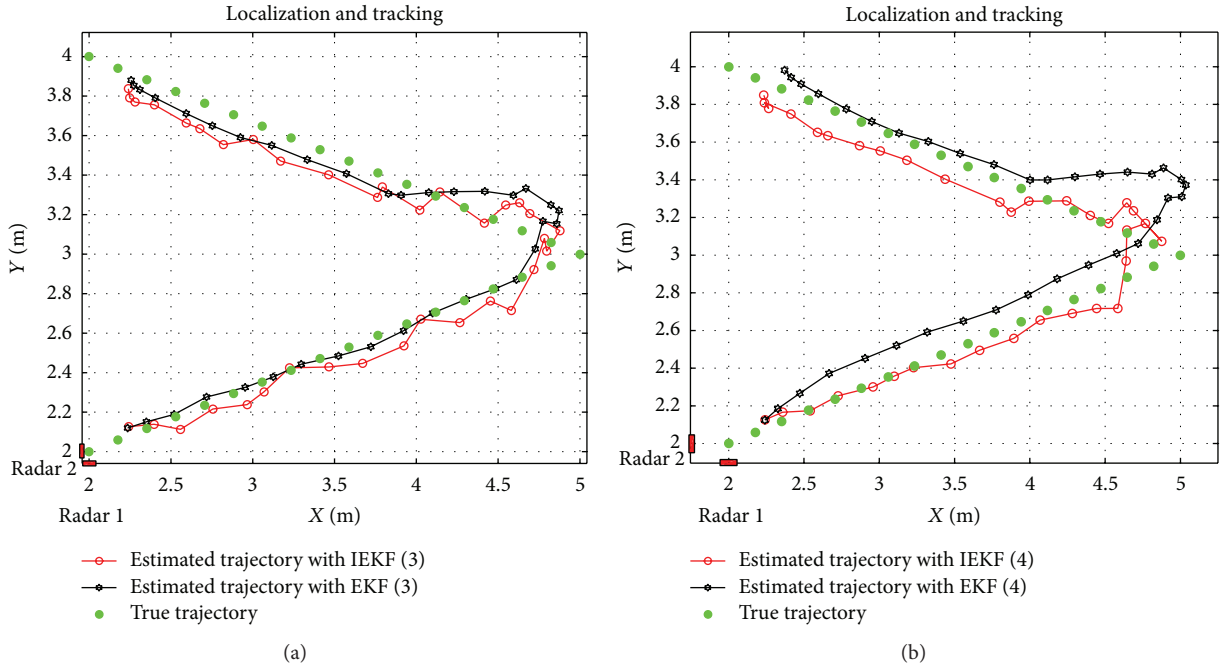


FIGURE 16: Estimated tracking result of moving target in 2D coordinates in the case of EKF and IEKF filtering methods, (a) EKF using  $c = 0.1$  and (b) EKF using  $c = 0.5$ .

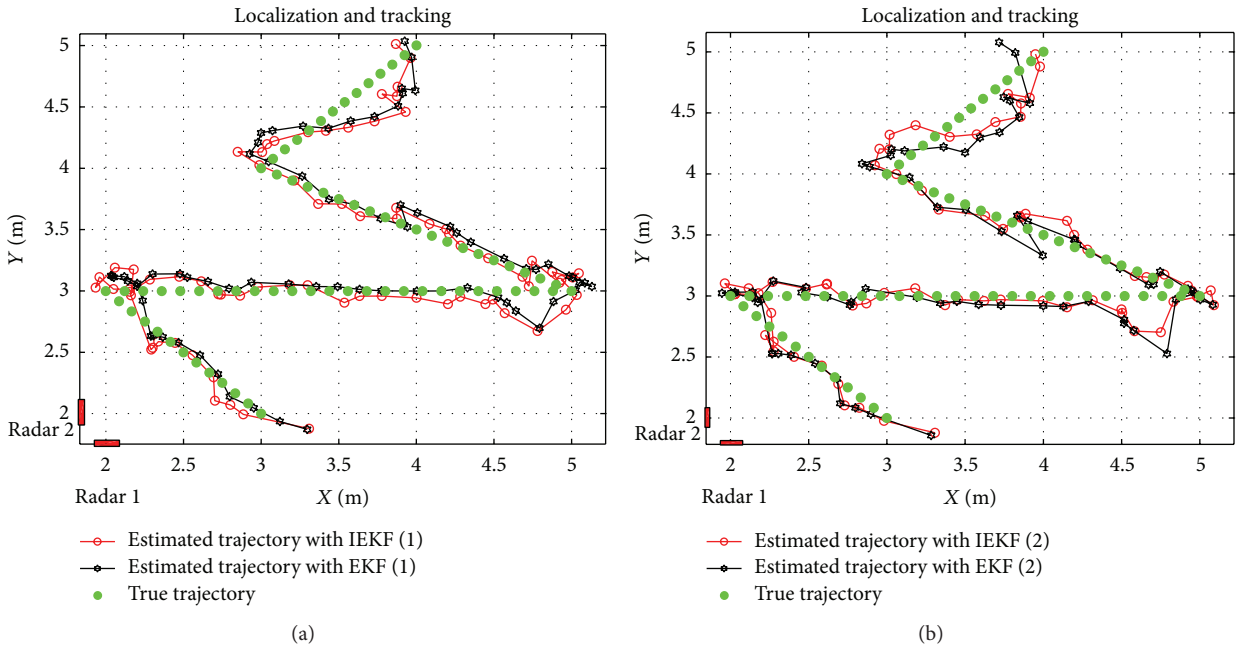


FIGURE 17: Estimated tracking result of moving target in 2D coordinates in the case of EKF and IEKF filtering methods, (a) EKF using  $c = 0.01$  and (b) EKF using  $c = 0.05$ .

most difficult procedure within IR-UWB signal processing. Even though the KF and EKF filter technologies have been used, there are still issues when enhancing the tracking accuracy. In this paper, we introduced the IEKF-based target tracking method, which can enhance the accuracy better than other conventional filters. Also, the detailed description about

experiment condition and parameters could be valuable in the incoming future 3D object tracking applications. In addition, for 2D radar tracking, the relation between position of radars and distance measurement is discussed in our paper. This IEKF-based tracking method can also be used in surveillance, rescue, and healthcare applications. If more

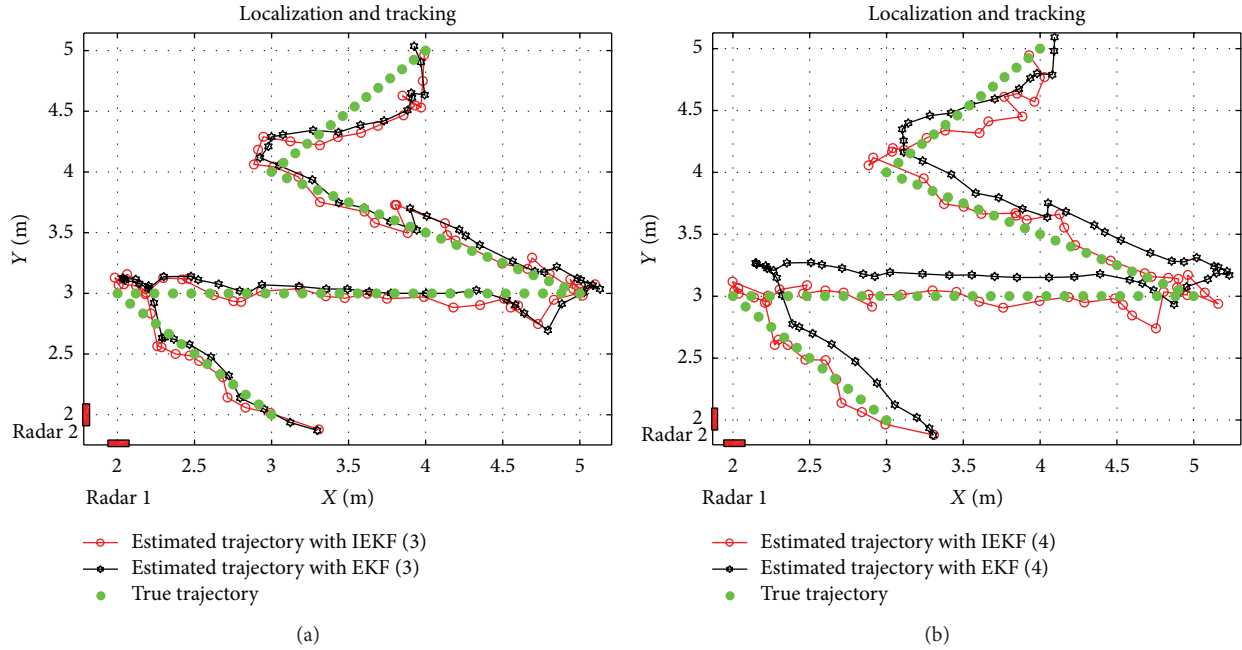


FIGURE 18: Estimated tracking result of moving target in 2D coordinates in the case of EKF and IEKF filtering methods, (a) EKF using  $c = 0.1$  and (b) EKF using  $c = 0.5$ .

TABLE 5: Performance comparison of different localization and tracking methods for trajectory case 2.

Method	RMSE	Covariance $R$
Without filtering	0.2526	None
EKF (1)	0.2378	$c = 0.01$
EKF (2)	0.2393	$c = 0.05$
EKF (3)	0.2336	$c = 0.1$
EKF (4)	0.3151	$c = 0.5$
IEKF (1)	0.2167	$c$ is randomly chosen
IEKF (2)	0.2198	$c$ is randomly chosen
IEKF (3)	0.2198	$c$ is randomly chosen
IEKF (4)	0.2145	$c$ is randomly chosen

radars are connected by wired and/or wireless links, multiple targets could be tracked with the lower location estimation errors in a larger area.

### Conflict of Interests

The authors declare that there is no conflict of interests regarding the publication of this paper.

### Acknowledgment

This research was supported by the Basic Science Research Program through the National Research Foundation of Korea (NRF) funded by the Ministry of Education, Science and Technology (no. 2014R1A1A2059952).

### References

- [1] N. Decarli, F. Guidi, and D. Dardari, "A novel joint RFID and radar sensor network for passive localization: design and performance bounds," *IEEE Journal on Selected Topics in Signal Processing*, vol. 8, no. 1, pp. 80–95, 2014.
- [2] I. I. Immoreev and P. G. S. D. V. Fedotov, "Ultra wideband radar systems: advantages and disadvantages," in *Proceedings of the IEEE Conference on Ultra Wideband Systems and Technologies. Digest of Papers*, pp. 201–205, Baltimore, Md, USA, May 2002.
- [3] R. J. Fontana, "Recent system applications of short-pulse ultra-wideband (UWB) technology," *IEEE Transactions on Microwave Theory and Techniques*, vol. 52, no. 9, pp. 2087–2104, 2004.
- [4] J. Rovnakova and D. Kocur, "UWB radar signal processing for through wall tracking of multiple moving targets," in *Proceedings of the European Radar Conference (EuRAD '10)*, pp. 372–375, IEEE, Paris, France, September–October 2010.
- [5] N. V. Han, D. M. Kim, G.-R. Kwon, and J.-Y. Pyun, "Clutter reduction on impulse radio ultra wideband radar signal," in *Proceedings of the International Technical Conference on Circuits/Systems, Computers and Communications (ITC-CSCC '13)*, no. 1, pp. 1091–1094, Sapporo, Japan, June 2013.
- [6] S. Singh, Q. L. Ling, D. C. Chen, and L. Sheng, "Sense through wall human detection using UWB radar," *EURASIP Journal on Wireless Communications and Networking*, vol. 2013, article 20, 11 pages, 2013.
- [7] N. V. Han and J.-Y. Pyun, "Improved target detection for moving object in IR-UWB radar," in *Proceedings of the International Conference on Green and Human Information Technology (ICGHIT '13)*, vol. 1, pp. 69–73, Hanoi, Vietnam, February 2013.
- [8] V.-H. Nguyen and J.-Y. Pyun, "Location detection and tracking of moving targets by a 2D IR-UWB radar system," *Sensors*, vol. 15, no. 3, pp. 6740–6762, 2015.

- [9] J. S. Park, I. S. Baek, and S. H. Cho, "Localizations of multiple targets using multistatic UWB radar systems," in *Proceedings of the 3rd IEEE International Conference on Network Infrastructure and Digital Content (IC-NIDC '12)*, pp. 586–590, Beijing, China, September 2012.
- [10] B. Sobhani, E. Paolini, A. Giorgetti, M. Mazzotti, and M. Chiani, "Target tracking for UWB multistatic radar sensor networks," *IEEE Journal of Selected Topics in Signal Processing*, vol. 8, no. 1, pp. 125–136, 2014.
- [11] B. H. Kim, H. J. Bae, S. Subedi, and J.-Y. Pyun, "Localization and tracking of moving target using iterative Kalman filter in 2D IR-UWB radar system," in *Proceedings of the SMA Meeting*, vol. 1, pp. 98–103, Savannah, Ga, USA, December 2014.
- [12] Novelda, *NVA6100 Preliminary Datasheet*, Novelda AS, 2011.
- [13] R. G. Brown and P. Y. C. Hwang, *Introduction to Random Signals and Applied Kalman Filtering*, John Wiley & Sons, New York, NY, USA, 3rd edition, 1996.
- [14] P. S. Maybeck, *Stochastic Models, Estimation, and Control*, vol. 2, Academic Press, New York, NY, USA, 1982.
- [15] Y. Bar-Shalom and X.-R. Li, *Estimation and Tracking Principles, Techniques and Software*, Artech House, Boston, Mass, USA, 1993.
- [16] J. D. Taylor and D. T. Wisland, "Novelda nanoscale impulse radar," in *Ultrawideband Radar: Applications and Design*, J. D. Taylor, Ed., pp. 373–388, CRC Press, New York, NY, USA, 1st edition, 2012.
- [17] C. L. Law, "Portable low-power IR-UWB system," in *Proceedings of the IEEE World Forum on Internet of Things (WF-IoT '14)*, pp. 474–478, Seoul, South Korea, March 2014.



**Hindawi**

Submit your manuscripts at  
<http://www.hindawi.com>

